Available online at www.sciencedirect.com
ScienceDirect
Journal of Sound and Vibration 298 (2006) 1034–1054
JOURNAL OF SOUND AND VIBRATION
www.elsevier.com/locate/jsvi

Free vibration of rotating tapered beams using the dynamic stiffness method

J.R. Banerjee*, H. Su, D.R. Jackson

School of Engineering and Mathematical Sciences, City University, Northampton Square, London EC1 V 0HB, UK

Received 8 February 2005; received in revised form 17 May 2006; accepted 5 June 2006
Available online 7 September 2006

Abstract

The free bending vibration of rotating tapered beams is investigated by using the dynamic stiffness method. The range of problems considered includes beams for which the depth and/or width of the cross-section vary linearly along the length. First, the governing differential equation of motion of the rotating tapered beam in free flap bending vibration is derived for the most general case using Hamilton's principle, allowing for the effects of centrifugal stiffening, an arbitrary outboard force and the hub radius term. For harmonic oscillation the differential equation is solved for bending displacement by applying the Frobenius method of series solution. The expressions for bending rotation, shear force and bending moment at any cross-section of the beam are also obtained in explicit analytical form. Then the dynamic stiffness matrix is developed, by relating the amplitudes of forces and moments to those of the displacements and rotations at the ends of the harmonically vibrating tapered beam. Next the Wittrick–Williams algorithm is used as a solution technique to the resulting dynamic stiffness matrix to compute the natural frequencies and mode shapes of some illustrative examples. A parametric study is carried out to demonstrate the effects of rotational speed, taper ratio and hub radius on the results, which are discussed and compared with the published ones. Finally some conclusions are drawn.

1. Introduction

The free vibration analysis of rotating uniform beams has been investigated more or less continuously over a long period and this is clearly evident from the literature. A few selective recent papers are quoted [1–4] which provide further references on the subject. By contrast, the free vibration analysis of rotating tapered beams appears to have been carried out relatively recently [4–8]. One of the reasons for this may be due to the fact that a tapered (or non-uniform) beam can be idealised as a collection of uniform beams to achieve sufficiently accurate results, without resorting to an in-depth original research. An example can be found in Ref. [4], which uses the dynamic stiffness theory of rotating uniform beams in order to analyse the free vibration behaviour of rotating tapered beams. The literature on the free vibration analysis of rotating beams shows that a wide range of different, but complementary methods has been used [9–15]. A significant contribution to the literature in recent years is the application of the dynamic stiffness method [4] to solve the

*Corresponding author. Tel.: +44 20 70408924; fax: +44 20 704 08566.
E-mail address: j.r.banerjee@city.ac.uk (J.R. Banerjee).

0022-460X/$ - see front matter © 2006 Elsevier Ltd. All rights reserved.
doi:10.1016/j.jsv.2006.06.040

Nomenclature

a_{i+1}	coefficients of Frobenius series, see Eqs. (22), (26)–(27), (29)–(30), (36)–(37)
$A(y)$	area of cross-section at a distance y from the origin
A_1–A_4	arbitrary constants used in series solution of Frobenius method, see Eq. (28)
c	taper ratio
C_1–C_{10}	non-dimensional beam parameters, see Eqs. (24) and (35)
$\bar{C}_1 - \bar{C}_7$	non-dimensional beam parameters, see Eq. (13)
E	Young's modulus of elasticity
EI_0	bending rigidity at the left-hand end (thick end) of the tapered beam
$\mathrm{EI}(y)$	bending rigidity of beam cross-section at a distance y from the origin
f	function used for the series obtained using the Frobenius method of solution
F_0	outboard force at the right-hand end (thin-end) of the tapered beam
$F(y)$	centrifugal force at a distance y from the origin
$\mathbf{F}$	amplitude of the force vector, see Eqs. (45)–(46) and (48)
$\mathbf{H}$	matrix defined in Eqs. (42) and (44)
k	parameter used in the Frobenius method to generate the indicial equation
$\mathbf{K}$	dynamic stiffness matrix, see Eqs. (48)–(49)
L	length of the tapered beam
m_0	mass per unit length at the left-hand end (thick end) of the tapered beam
$m(y)$	mass per unit length of beam cross-section at a distance y from the origin
M	bending moment
n	integer defining the type of taper, see Eqs. (1) and (2), n is either 1 or 2
$\mathbf{Q}$	matrix defined in Eqs. (45) and (47)
r_H	hub radius
S	shear force
T	kinetic energy of the rotating tapered beam
U	potential energy of the rotating tapered beam
w	transverse or flap wise bending displacement
W	amplitude of transverse or flap wise bending displacement
X, Y, Z	rectangular Cartesian coordinate system
δ	variational operator
$\boldsymbol{\delta}$	displacement vector
ζ	non-dimensional variable defined in Eq. (18)
η	non-dimensional rotational speed, see Eq. (50)
θ	bending rotation
λ_i	non-dimensional natural frequencies, see Eqs. (50) and (51)
ξ	non-dimensional length defined in Eq. (11)
ρ	mass density of material
ω	circular or angular frequency

free vibration problem of rotating beams. There are other research papers on rotating Timoshenko beams [16–18], but this particular subject matter is outside the scope of the present paper, which uses the Bernoulli–Euler theory.

An important reason for using the dynamic stiffness method is that it gives exact results for all natural frequencies and mode shapes, without making any approximation en route [19]. This is possible because the method uses exact member theory based on frequency-dependant shape functions obtained from the solution of the governing differential equations of motion of the structural element undergoing free vibration. Thus the dynamic stiffness method has always been distinctive and is used with advantage wherever possible, for example, in validating the finite element and other approximate methods. It is well known that the finite element and other approximate methods become more and more unreliable at higher frequencies. Furthermore, one of the great advantages of the dynamic stiffness method is that the results are independent of the number of elements used in the analysis. For instance, one single structural element can be used to obtain any number of its natural frequencies and mode shapes to any desired accuracy. This is clearly impossible in the finite element and other approximate methods in which the results are generally, if not always, dependant on the number and quality of the elements used in the analysis. This has in part motivated the current work, which sets out to derive the dynamic stiffness matrix of a rotating tapered beam and then to use it to investigate its free vibration characteristics.

The range of problems considered includes beams with linearly varying taper in depth and/or width of the cross-section along the length. In terms of cross-sectional properties this essentially means that the area and the second moment of area of the beam can vary in two different ways. In the case when either the depth or the width (but not both) of the beam varies linearly along the length, the corresponding variation of the area of cross-section will be linear whereas the variation of the second moment of area will be cubic. On the other hand when both the depth and the width vary linearly, the variation of the cross-sectional area will follow a square law whereas the second moment of area variation will be of fourth power. Using these two types of property variations, a large number of cross-sections can be constructed [20,21], which cover a large number of practical cases. For instance, a linearly varying tapered beam with thin-walled circular cross-section of constant thickness falls in the former category whereas the one with a solid circular cross-section will belong to the latter.

For validation purposes the availability of essential numerical results from independent sources is important, particularly for the present study, which uses an exact dynamic stiffness theory and is specially aimed to establish benchmark solutions to the problem. In this respect, there are some published numerical results with high degree of accuracy [7] for the free vibration problem of rotating tapered beams of the former type, dealing with linear variation of the area and cubic variation of the second moment of area. However, for the latter type of problems for which the area and the second moment of area of the cross-section follow, respectively, a square and fourth power law, Khulief [8] appears to be the only author who reported detailed numerical results with sufficient number of significant figures, covering a wide range. During the course of the present investigation the work of Khulief [8] was given due recognition, but unfortunately, it was observed that the results are somehow inaccurate. The present authors spent considerable time in checking their theory with the (perceived) understanding that the published results of Ref. [8] were sufficiently accurate. Having expended a great deal of effort in checking the theory and associated computer programs, the authors carried out an additional finite element analysis of the problem alongside their dynamic stiffness work. Furthermore, an independent confirmation of the correctness of the authors' results came from a private communication [22], which provided some further stimulus to the research. A brief synopsis of the work is as follows.

Starting from the derivation of the governing differential equations of motion in free vibration, using Hamilton's principle, the dynamic stiffness matrix of a harmonically vibrating tapered beam is developed for a general case with the effects of hub radius and the centrifugal force taken into account. The dynamic stiffness matrix is then applied with particular reference to the Wittrick–William algorithm [23], yielding natural frequencies and mode shapes of some examples. The numerical results are discussed and compared with published ones.

2. Theory

The two types of rotating tapered beams considered in this paper are shown in Figs. 1 and 2, respectively, in a right-handed Cartesian coordinate system with the Y-axis coinciding with the axis of the beam. The Z-axis is taken to be parallel, but not coincidental with the axis of rotation. It is assumed that the tapered beam is rotating at a constant angular velocity Ω with an arbitrary hub radius r_H as shown. The tapered beam shown in Fig. 1 displays a linear variation of depth and a constant width of the cross-section along the length whereas the one in Fig. 2 shows a linear variation of both width and depth. Clearly for the former the variations of cross-sectional area and second moment of area are linear and cubic whereas those for the latter are of second and fourth order, respectively.

If L is the length, c is the taper ratio, $A(y)$ and $I(y)$ are the area and second moment of area of the cross-section at a distance y, and ρ and E are the density and Young's modulus of the (isotropic) beam material, respectively, then the variations of the mass per unit length $m(y)$, and the bending rigidity $\mathrm{EI}(y)$ for both types of tapered beam can be expressed by using the following formulas:

$$m(y) = \rho A(y) = m_0\left(1 - c\frac{y}{L}\right)^n \tag{1}$$

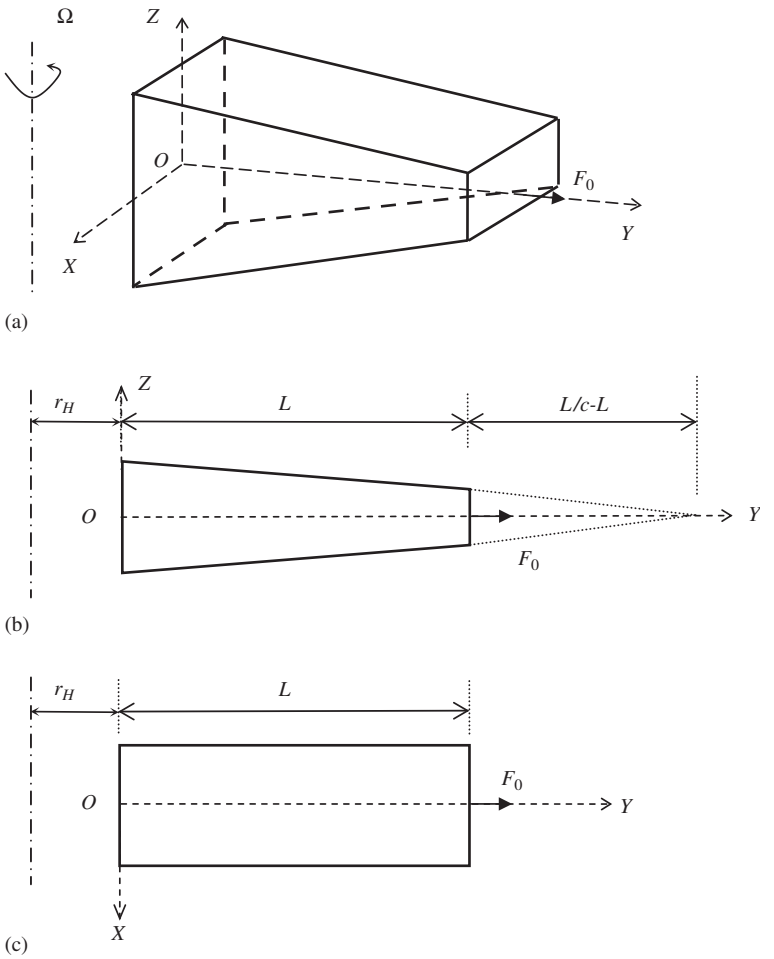

Fig. 1. A rotating tapered beam with a constant width and a linearly varying depth for which the variations of the cross-sectional area and the second moment of area along the length are linear and cubic, respectively: (a) pictorial view, (b) front elevation, (c) plan.

and

$$\mathrm{EI}(y) = \mathrm{EI}_0\left(1 - c\frac{y}{L}\right)^{n+2}, \tag{2}$$

where m_0 and EI_0 are the mass per unit length and the flexural rigidity at the left-hand end of the beam, respectively. The integer n takes the value 1 for the first type (see Fig. 1) and 2 for the second type (see Fig. 2) of tapered beams described by Eqs. (1) and (2). A large number of cross-sections can be constructed by using these two values of n (see Refs. [20,21]), covering many practical cases. However, the rectangular cross-section is shown in Figs. 1 and 2 only for convenience. (It is evident that for such a cross-section, if one of the dimensions, say, the depth, is varied linearly and the other, say width, is kept constant, the value of n will be equal to 1 whereas if both the dimensions are varied linearly, n will take the value 2.)

The taper ratio c is such that $0 < c < 1$, see Figs. 1 and 2. Clearly, when $c = 0$ the beam is uniform for which the dynamic stiffness theory has already been developed [4]. However, when $c = 1$, the beam tapers to a point which makes the elastic critical buckling load of the beam zero [24,25]. Of course, $c = 1$, is a theoretical limit which can never be reached in practice even though the natural frequencies of this limiting case have been reported in the literature [26]. Furthermore, the theory presupposes that the shear centre and centroid of the beam cross-section are coincident so that there is no torsional coupling induced by the bending motion. Any other form of coupling through Coriolis forces is also neglected. The beam is assumed to behave according to the Bernoulli–Euler theory and only the flapping motion is considered in the analysis.

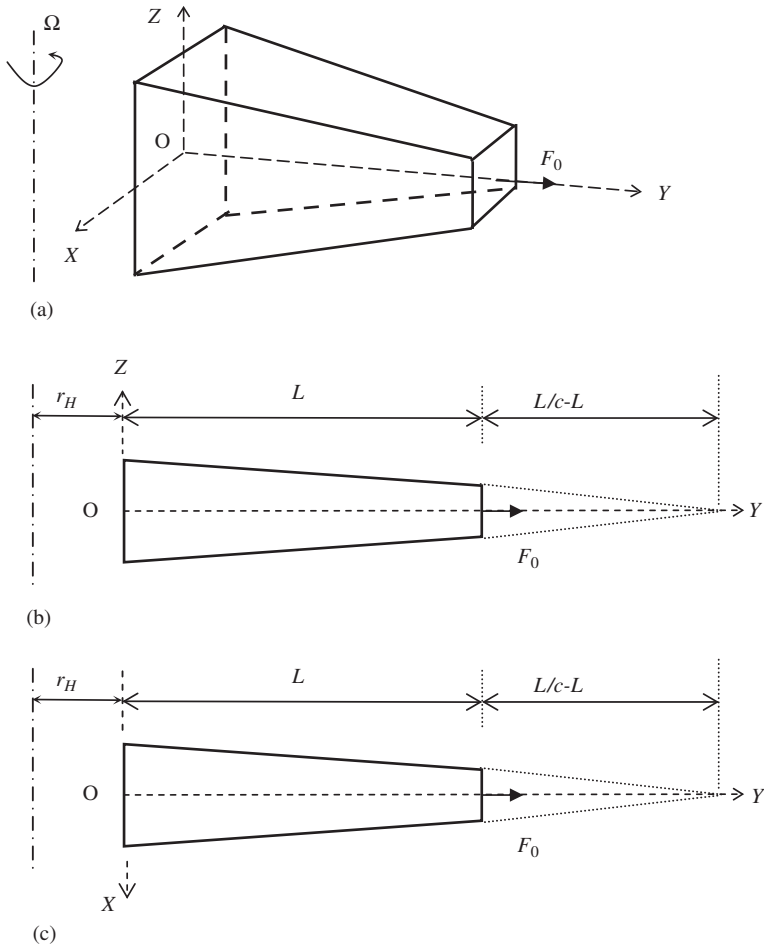

Fig. 2. A rotating tapered beam with linearly varying width and depth for which the variations of the cross-sectional area and the second moment of area along the length are second and fourth order, respectively: (a) pictorial view, (b) front elevation, (c) plan.

2.1. Derivation of the governing differential equations of motion

The governing differential equations of motion of the rotating tapered beam in free vibration are derived for the general case, see Eqs. (1) and (2), by applying Hamilton's principle which requires the expressions for potential (or strain) and kinetic energies of the beam as fundamental prerequisites.

The potential or strain energy U of the beam is given by

$$U = \frac{1}{2}\int_0^L \mathrm{EI}(y)(w'')^2\,\mathrm{d}y + \frac{1}{2}\int_0^L F(y)(w')^2\,\mathrm{d}y, \tag{3}$$

where w is the transverse displacement (in the Z-direction, see Figs. 1 and 2), a prime denotes differentiation with respect to y, and $F(y)$ is the centrifugal force at a distance y from the root cross-section of the beam, arising from the rotating action.

The centrifugal force $F(y)$ can be expressed as

$$F(y) = \int_y^L m(y)\Omega^2(r_H + y)\,\mathrm{d}y + F_0, \tag{4}$$

where F_0 is an outboard force at the right-hand end of the beam, as shown in Figs. 1 and 2. (In order to make the theory sufficiently general, this outboard force F_0, which is zero when the right-hand end is completely free, is necessary [4], e.g. when assembling dissimilar rotating tapered beams rigidly joined together.)

The kinetic energy T of the beam is given by

$$T = \frac{1}{2}\int_0^L m(y)\dot{w}^2\,\mathrm{d}y, \tag{5}$$

where an over dot represents differentiation with respect to time t.

Hamilton's principle states

$$\delta\int_{t_1}^{t_2}(T-U)\,\mathrm{d}t = 0, \tag{6}$$

where t_1 and t_2 are the time intervals in the dynamic trajectory, and δ is the usual variational operator.

Substituting for T and U, from Eqs. (3) and (5) into Eq. (6), using the δ operator, integrating each term by parts, and then collecting terms give the following governing differential equation in free vibration for the rotating tapered beam:

$$(\mathrm{EI}w'')'' - (Fw')' + m\ddot{w} = 0. \tag{7}$$

As a by-product of the Hamiltonian formulation the natural boundary conditions give the expressions for shear force and bending moment as follows:

$$S = (\mathrm{EI}w'')' - Fw', \tag{8}$$

$$M = -\mathrm{EI}w''. \tag{9}$$

Assuming harmonic oscillation so that

$$w(y,t) = W(y)\cos\omega t, \tag{10}$$

where W is the amplitudes of w, and ω the angular or circular frequency of oscillation.

Introducing the non-dimensional length ξ, where

$$\xi = 1 - c\frac{y}{L} \tag{11}$$

the governing differential equation (7), on substitutions of Eqs. (4), (10) and (11) and after some simplification becomes

$$\begin{aligned}&\xi^{n+2}W'''' + 2(n+2)\xi^{n+1}W''' + (\bar{C}_1\xi^{n+2} + \bar{C}_2\xi^{n+1} + \bar{C}_3\xi^n + \bar{C}_4)W''\\ &\quad + (\bar{C}_5\xi^{n+1} + \bar{C}_6\xi^n)W' - \bar{C}_7\xi^n W = 0,\end{aligned} \tag{12}$$

where a prime here denotes differentiation with respect to ξ, and $\bar{C}_1, \bar{C}_2, \ldots, \bar{C}_7$ are non-dimensional parameters defined as follows:

$$\begin{aligned}&\bar{C}_1 = \frac{m_0\Omega^2L^4}{\mathrm{EI}_0c^4(n+2)},\ \bar{C}_2 = -\frac{m_0\Omega^2L^3}{EI_0c^3(n+1)}\left(r_H + \frac{L}{c}\right),\ \bar{C}_3 = (n+1)(n+2),\\ &\bar{C}_4 = -\bar{C}_1(1-c)^{n+2} - \bar{C}_2(1-c)^{n+1} - \frac{F_0L^2}{\mathrm{EI}_0c^2},\ \bar{C}_5 = \frac{m_0\Omega^2L^4}{\mathrm{EI}_0c^4},\\ &\bar{C}_6 = -\frac{m_0\Omega^2L^3}{\mathrm{EI}_0c^3}\left(r_H + \frac{L}{c}\right),\ \bar{C}_7 = \frac{m_0\omega^2L^4}{\mathrm{EI}_0c^4}.\end{aligned} \tag{13}$$

The shear force and bending moment can also be expressed in terms of the new variable ξ as follows:

$$S(\xi) = R_3[\xi^{n+2}W''' - (n+2)\xi^{n+1}W'' + (\bar{C}_1\xi^{n+2} + \bar{C}_2\xi^{n+1} + \bar{C}_4)W'], \tag{14}$$

$$M(\xi) = -R_2\xi^{n+2}W'', \tag{15}$$

where

$$R_2 = \mathrm{EI}_0 \frac{c^2}{L^2},\ R_3 = \mathrm{EI}_0 \frac{c^3}{L^3}. \tag{16}$$

The centrifugal force, after substitution of Eqs. (1) and (11) into Eq. (4), can be written in terms of ξ as

$$F(\xi) = \frac{-m_0\Omega^2 L}{c(n+1)(n+2)}\left[(n+2)\left(r_H + \frac{L}{c}\right)\{(1-c)^{n+1} - \xi^{n+1}\} - \frac{L}{c}(n+1)\{(1-c)^{n+2} - \xi^{n+2}\}\right] + F_0. \tag{17}$$

The differential equation (12) is linear, but has variable coefficients and is amenable to Frobenius method of series solution. As it will be shown later, the introduction of a further new variable ζ is proved to be helpful in obtaining the roots of the indicial equation in simple form (similar to those obtained for rotating uniform beams), which facilitates an easy and straightforward application of the series solution. Substituting

$$\zeta = 1 - \xi \tag{18}$$

the governing differential equation (12) becomes

$$\begin{aligned}(1-\zeta)^{n+2}W'''' + 2(n+2)(1-\zeta)^{n+1}W''' + \{\bar{C}_1(1-\zeta)^{n+2} + \bar{C}_2(1-\zeta)^{n+1} + \bar{C}_3(1-\zeta)^n + \bar{C}_4\}W'' \\ + \{\bar{C}_5(1-\zeta)^{n+1} + \bar{C}_6(1-\zeta)^n\}W' - \bar{C}_7(1-\zeta)^n W = 0,\end{aligned} \tag{19}$$

where a prime here denotes differentiation with respect to ζ. Similarly, the shear force and bending moment can be written in terms of the new variable ζ as follows:

$$S(\zeta) = R_3[(1-\zeta)^{n+2}W''' - (n+2)(1-\zeta)^{n+1}W'' + \{\bar{C}_1(1-\zeta)^{n+2} + \bar{C}_2(1-\zeta)^{n+1} + \bar{C}_4\}W'], \tag{20}$$

$$M(\zeta) = -R_2(1-\zeta)^{n+2}W''. \tag{21}$$

Note that the Eqs. (19)–(21) are valid for both types of tapered beam ($n = 1$ or 2). Of course, the coefficients of the differential equation (19) and the expressions for shear force and bending moment given by Eqs. (20) and (21) will be different for the two cases when n is substituted as 1 or 2.

2.2. Frobenius method of solution

The exact solution of the governing differential equation (19) can be obtained in series form, using the Frobenius method [27]. In this method, when seeking the solution, a power (infinite) series in terms of the independent variable (in this case ζ) is substituted in the differential equation, which is followed by the determination of the roots of the indicial equation and finally the evaluation of the constants. Thus, the solution W of the differential equation (19) can be expressed as

$$W(\zeta, k) = \sum_{i=0}^{\infty} a_{i+1}(k)\zeta^{k+i}, \tag{22}$$

where k and the coefficients a_{i+1} are unknown and need to be determined such that $W(\zeta, k)$ is the solution of Eq. (19).

Because of the nature of the differential equation (19) it is now necessary to solve each of the two cases corresponding to $n = 1$ and 2 separately.

2.2.1. Solution for the case when $n = 1$

Substitution of $n = 1$ into Eq. (19) and after some simplification, one obtains

$$\begin{aligned}(\zeta^3 - 3\zeta^2 + 3\zeta - 1)W'''' + 6(\zeta^2 - 2\zeta + 1)W''' \\ + (C_1\zeta^3 + C_2\zeta^2 + C_3\zeta + C_4)W'' + (C_5\zeta^2 + C_6\zeta + C_7)W' \\ + C_8(\zeta - 1)W = 0,\end{aligned} \tag{23}$$

where

$$C_1 = \bar{C}_1,\ C_2 = -(3\bar{C}_1 + \bar{C}_2),\ C_3 = 3\bar{C}_1 + 2\bar{C}_2 + \bar{C}_3,$$
$$C_4 = -(\bar{C}_1 + \bar{C}_2 + \bar{C}_3 + \bar{C}_4),\ C_5 = \bar{C}_5,\ C_6 = -(2\bar{C}_5 + \bar{C}_6),$$
$$C_7 = \bar{C}_5 + \bar{C}_6,\ C_8 = -\bar{C}_7 \tag{24}$$

and $\bar{C}_1 - \bar{C}_7$ are given by Eq. (13) when $n = 1$.

Substituting Eq. (22) into Eq. (23) yields the following indicial Eq. (27):

$$k(k-1)(k-2)(k-3) = 0. \tag{25}$$

Clearly, the roots of the indicial equation are 0, 1, 2, 3, which are all distinct and separate integers. Note that the indicial Eq. (25) has turned out to be exactly the same as the one encountered in a uniform rotating beam [4,16]. (This has been possible because the variable ξ was changed to ζ where $\zeta = 1-\xi$.)

Using standard procedure [27] the recurrence relationship which determines the coefficient terms for each of the four roots of the indicial equation can be expressed as

$$\begin{aligned} a_{i+5}(k) = {} & 3\frac{(k+i+2)}{(k+i+4)}a_{i+4} - \frac{3(k+i)(k+i-1)+12(k+i)-C_4}{(k+i+4)(k+i+3)}a_{i+3} \\ & + \frac{(k+i)(k+i-1)(k+i-2)+6(k+i)(k+i-1)+C_3(k+i)+C_7}{(k+i+4)(k+i+3)(k+i+2)}a_{i+2} \\ & + \frac{C_2(k+i)(k+i-1)+C_6(k+i)-C_8}{(k+i+4)(k+i+3)(k+i+2)(k+i+1)}a_{i+1} \\ & + \frac{C_1(k+i-1)(k+i-2)+C_5(k+i-1)+C_8}{(k+i+4)(k+i+3)(k+i+2)(k+i+1)}a_i, \end{aligned} \tag{26}$$

where

$$\begin{aligned} a_1 &= 1,\ a_2 = \frac{3(k-1)}{(k+1)}a_1, \\ a_3 &= \frac{3k}{(k+2)}a_2 - \frac{3(k-2)(k-3)+12(k-2)-C_4}{(k+2)(k+1)}a_1, \\ a_4 &= \frac{3(k+1)}{k+3}a_3 - \frac{3(k-1)(k-2)+12(k-1)-C_4}{(k+3)(k+2)}a_2 \\ &\quad + \frac{(k-1)(k-2)(k-3)+6(k-1)(k-2)+C_3(k-1)+C_7}{(k+3)(k+2)(k+1)}a_1, \\ a_5 &= \frac{3(k+2)}{(k+4)}a_4 - \frac{3k(k-1)+12k-C_4}{(k+4)(k+3)}a_3 + \frac{k(k-1)(k-2)+6k(k-1)+C_3k+C_7}{(k+4)(k+3)(k+2)}a_2 \\ &\quad + \frac{C_2k(k-1)+C_6k-C_8}{(k+4)(k+3)(k+2)(k+1)}a_1. \end{aligned} \tag{27}$$

The solution of the governing differential equation of motion can now be expressed as a combination of four linear solutions multiplied by four arbitrary constants as follows:

$$W(\zeta) = A_1 f(\zeta,\ 0) + A_2 f(\zeta,\ 1) + A_3 f(\zeta,\ 2) + A_4 f(\zeta,\ 3), \tag{28}$$

where A_1, A_2, A_3 and A_4 are the four arbitrary constants and

$$f(\zeta,\ k) = \sum_{i=0}^{\infty} a_{i+1}(k)\zeta^{k+i} \tag{29}$$

with $k = 0$, 1, 2 and 3.

The four independent solutions $f(\zeta, k)$ for $k = 0, 1, 2$ and 3, can be expanded using the first few terms as follows:

$$\begin{aligned} f(\zeta, 0) &= a_1(0) + a_2(0)\zeta + a_3(0)\zeta^2 + a_4(0)\zeta^3 + a_5(0)\zeta^4 + \cdots \\ f(\zeta, 1) &= a_1(1)\zeta + a_2(1)\zeta^2 + a_3(1)\zeta^3 + a_4(1)\zeta^4 + a_5(1)\zeta^5 + \cdots \\ f(\zeta, 2) &= a_1(2)\zeta^2 + a_2(2)\zeta^3 + a_3(2)\zeta^4 + a_4(2)\zeta^5 + a_5(2)\zeta^6 + \cdots \\ f(\zeta, 3) &= a_1(3)\zeta^3 + a_2(3)\zeta^4 + a_3(3)\zeta^5 + a_4(3)\zeta^6 + a_5(3)\zeta^7 + \cdots \quad . \end{aligned} \tag{30}$$

With the help of Eqs. (28), (20) and (21), the expressions for the bending rotation θ, shear force S and bending moment M are, respectively, given by

$$\theta(\zeta) = \frac{c}{L}\frac{\mathrm{d}W}{\mathrm{d}\zeta} = \frac{c}{L}\left[A_1 f'(\zeta, 0) + A_2 f'(\zeta, 1) + A_3 f'(\zeta, 2) + A_4 f'(\zeta, 3)\right], \tag{31}$$

$$S(\zeta) = R_3[(1-\zeta)^3 W''' - 3(1-\zeta)^2 W'' + \{\bar{C}_1(1-\zeta)^3 + \bar{C}_2(1-\zeta)^2 + \bar{C}_4\}W'], \tag{32}$$

$$M(\zeta) = -R_2(1-\zeta)^3 W''. \tag{33}$$

2.2.2. Solution for the case when $n = 2$

The differential equation for the case $n = 2$ follows from Eq. (19) and takes the following form:

$$\begin{aligned} &(\zeta^4 - 4\zeta^3 + 6\zeta^2 - 4\zeta + 1)W'''' + 8(\zeta^3 - 3\zeta^2 + 3\zeta - 1)W''' \\ &\quad + (C_1\zeta^4 + C_2\zeta^3 + C_3\zeta^2 + C_4\zeta + C_5)W'' + (C_6\zeta^3 + C_7\zeta^2 + C_8\zeta + C_9)W' \\ &\quad + C_{10}(\zeta^2 - 2\zeta + 1)W = 0 \end{aligned} \tag{34}$$

with

$$\begin{aligned} C_1 &= \bar{C}_1 & C_2 &= -(4\bar{C}_1 + \bar{C}_2), \\ C_3 &= 6\bar{C}_1 + 3\bar{C}_2 + \bar{C}_3 & C_4 &= -(4\bar{C}_1 + 3\bar{C}_2 + 2\bar{C}_3), \\ C_5 &= \bar{C}_1 + \bar{C}_2 + \bar{C}_3 + \bar{C}_4 & C_6 &= \bar{C}_5, \\ C_7 &= -(3\bar{C}_5 + \bar{C}_6) & C_8 &= 3\bar{C}_5 + 2\bar{C}_6, \\ C_9 &= -(\bar{C}_5 + \bar{C}_6) & C_{10} &= -\bar{C}_7, \end{aligned} \tag{35}$$

where $\bar{C}_1 - \bar{C}_7$ are given by Eq. (13) when $n = 2$.

The differential equation (34) can be solved in a similar manner to that of the previous Eq. (23) when n was 1. The indicial equation takes exactly the same form as Eq. (25) and yields the roots $k = 0, 1, 2, 3$, as before, but of course, the final solution will be different because the coefficient terms $a_{i+1}(k)$ in Eq. (22) are different. The recurrence relationship for this case when $n = 2$, is given by

$$\begin{aligned} a_{i+6} = {} & 4\frac{(k+i+3)}{(k+i+5)}a_{i+5} - \frac{6(k+i+1)(k+i) + 24(k+i+1) + C_5}{(k+i+5)(k+i+4)}a_{i+4} \\ & + \frac{4(k+i+1)(k+i)(k+i-1) + 24(k+i+1)(k+i) - C_4(k+i+1) - C_9}{(k+i+5)(k+i+4)(k+i+3)}a_{i+3} \\ & - \frac{(k+i+1)(k+i)(k+i-1)(k+i+6) + C_3(k+i+1)(k+i) + C_8(k+i+1) + C_{10}}{(k+i+5)(k+i+4)(k+i+3)(k+i+2)}a_{i+2} \\ & - \frac{C_2(k+i)(k+i-1) + C_7(k+i) - 2C_{10}}{(k+i+5)(k+i+4)(k+i+3)(k+i+2)}a_{i+1} \\ & - \frac{C_1(k+i-1)(k+i-2) + C_6(k+i-1) + C_{10}}{(k+i+5)(k+i+4)(k+i+3)(k+i+2)}a_i, \end{aligned} \tag{36}$$

where

$$
\begin{aligned}
a_1 &= 1,\ a_2 = \frac{4(k-1)}{(k+1)}a_1,\ a_3 = \frac{4k}{(k+2)}a_2 - \frac{6(k-2)(k-3)+24(k-2)+C_5}{(k+2)(k+1)}a_1,\\
a_4 &= \frac{4(k+1)}{k+3}a_3 - \frac{6(k-1)(k-2)+24(k-1)+C_5}{(k+3)(k+2)}a_2\\
&\quad + \frac{4(k-1)(k-2)(k-3)+24(k-1)(k-2)-C_4(k-1)-C_9}{(k+3)(k+2)(k+1)}a_1,\\
a_5 &= \frac{4(k+2)}{k+4}a_4 - \frac{6k(k-1)+24k+C_5}{(k+4)(k+3)}a_3 + \frac{4k(k-1)(k-2)+24k(k-1)-C_4k-C_9}{(k+4)(k+3)(k+2)}a_2\\
&\quad - \frac{k(k-1)(k-2)(k-3)+8k(k-1)(k-2)+C_3k(k-1)+C_8k+C_{10}}{(k+4)(k+3)(k+2)(k+1)}a_1,\\
a_6 &= \frac{4(k+3)}{(k+5)}a_5 - \frac{6k(k+1)+24(k+1)+C_5}{(k+5)(k+4)}a_4\\
&\quad + \frac{4k(k+1)(k-1)+24k(k+1)-C_4(k+1)-C_9}{(k+5)(k+4)(k+3)}a_3\\
&\quad - \frac{k(k+1)(k-1)(k-2)+8k(k+1)(k-1)+C_3k(k+1)+C_8(k+1)+C_{10}}{(k+5)(k+4)(k+3)(k+2)}a_2\\
&\quad - \frac{c_2k(k-1)+C_7k-2C_{10}}{(k+5)(k+4)(k+3)(k+2)}a_1.
\end{aligned}
\tag{37}
$$

Note that a_i ($i = 1, 2, \ldots 6$) above are all functions of k as in the case $n = 1$. The solution of the governing differential equation for $n = 2$ can now be expressed exactly in the same way as Eq. (28), but with different sets of four solutions $f(\zeta, k)$ obtained by using the recurrence relationship given by Eq. (36). The expression for the bending rotation θ will have the same form as Eq. (31), but of course, will now contain different expressions for $f'(\zeta, k)$. The expressions for shear force S and bending moment M follow from Eqs. (20) and (21), and are, respectively, given by

$$S(\zeta) = R_3[(1-\zeta)^4 W''' - 4(1-\zeta)^3 W'' + \{\bar{C}_1(1-\zeta)^4 + \bar{C}_2(1-\zeta)^3 + \bar{C}_4\}W'], \tag{38}$$

$$M(\zeta) = -R_2(1-\zeta)^4 W''. \tag{39}$$

2.3. Formulation of the dynamic stiffness matrix

Having developed the expressions for bending displacement (W), bending rotation (θ), shear force (S) and bending moment (M), the dynamic stiffness matrix can now be formulated by applying the boundary conditions for both cases.

Following the sign convention shown in Fig. 3 for positive shear force and bending moment and referring to Fig. 4, the boundary conditions for the displacements and forces (for each of the two cases, i.e., $n = 1$ and 2) are given as follows:

Displacements:

$$
\begin{aligned}
&\text{At} \quad y = 0 \text{ (i.e. } \xi = 1 \text{ or } \zeta = 0): \ W = W_1;\ \theta = \theta_1,\\
&\text{At} \quad y = L \text{ (i.e. } \xi = 1 - c \text{ or } \zeta = c): \ W = W_2;\ \theta = \theta_2.
\end{aligned}
\tag{40}
$$

Forces:

$$
\begin{aligned}
&\text{At} \quad y = 0 \text{ (i.e. } \xi = 1 \text{ or } \zeta = 0): \ S = S_1;\ M = M_1,\\
&\text{At} \quad y = L \text{ (i.e. } \xi = 1 - c \text{ or } \zeta = c): \ S = -S_2;\ M = -M_2.
\end{aligned}
\tag{41}
$$

Substituting Eq. (40) into Eqs. (28) and (31) gives the following matrix relationship. (Note that Eqs. (28) and (31) are applicable to both cases for $n = 1$ and 2)

$$\boldsymbol{\delta} = \mathbf{H}\mathbf{A}, \tag{42}$$

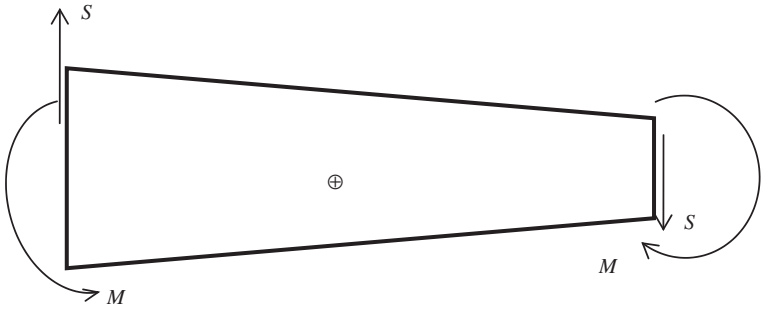

Fig. 3. Sign convention for positive shear force (S) and positive bending moment (M).

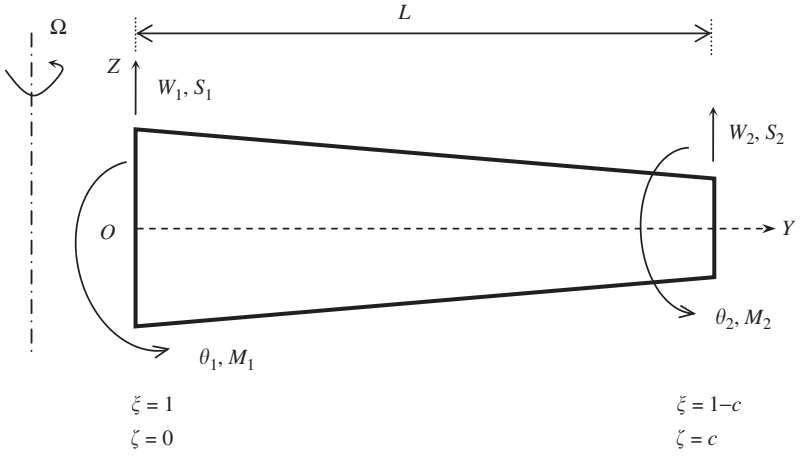

Fig. 4. Boundary conditions for displacements and forces.

where

$$\boldsymbol{\delta} = [W_1 \theta_1 W_2 \theta_2]^{\mathrm{T}}, \qquad \mathbf{A} = [A_1 A_2 A_3 A_4]^{\mathrm{T}} \tag{43}$$

and

$$\mathbf{H} = \begin{bmatrix} a_1(0) & 0 & 0 & 0 \\ \frac{c}{L}a_2(0) & \frac{c}{L}a_1(1) & 0 & 0 \\ f(c,\,0) & f(c,\,1) & f(c,\,2) & f(c,\,3) \\ \frac{c}{L}f'(c,\,0) & \frac{c}{L}f'(c,\,1) & \frac{c}{L}f'(c,\,2) & \frac{c}{L}f'(c,\,3) \end{bmatrix}. \tag{44}$$

Note that the upper suffix T in Eq. (43) denotes a transpose, and the elements a_i and $f(c,i)$ of the matrix $\mathbf{H}$ in Eq. (44) are different for the two cases with $n = 1$ and 2 (see Eqs. (27), (30) and (37)).

Similarly, substituting Eq. (41) into Eqs. (32), (33) for $n = 1$, and into (38), (39) for $n = 2$ gives the following matrix relationship:

$$\mathbf{F} = \mathbf{Q}\mathbf{A}, \tag{45}$$

where the column matrix $\mathbf{A}$ (i.e. the vector of constants $A_1 - A_4$) has already been defined in Eq. (43) and

$$\mathbf{F} = [S_1 M_1 S_2 M_2]^{\mathrm{T}} \tag{46}$$

and the matrix **Q** is expressed as follows:

$$\mathbf{Q} = \begin{bmatrix} q_{11} & q_{12} & q_{13} & q_{14} \\ q_{21} & q_{22} & q_{23} & q_{24} \\ q_{31} & q_{32} & q_{33} & q_{34} \\ q_{41} & q_{42} & q_{43} & q_{34} \end{bmatrix}. \tag{47}$$

The elements of **Q** matrix, $q_{ij}(i = 1, 2, \ldots 4, j = 1, 2, \ldots 4)$ obtained from the expressions for shear force and bending moment, are different for the two cases as expected, and these are given in Appendix A. Note that the column vectors for nodal displacements $\boldsymbol{\delta}$, nodal forces **F**, and the constants **A**, are represented by their respective transposes in order to save space.

The dynamic stiffness matrix of the rotating tapered beam **K** can now be derived by eliminating the constant vector **A** from Eqs. (42) and (45) and thus relating the amplitudes of the forces **F** to those of the displacements $\boldsymbol{\delta}$ at the ends of the harmonically vibrating rotating tapered beam. In matrix notation, this is represented by

$$\mathbf{F} = \mathbf{K}\boldsymbol{\delta}, \tag{48}$$

where

$$\mathbf{K} = \mathbf{Q}\mathbf{H}^{-1} \tag{49}$$

is the required frequency dependant dynamic stiffness matrix of the rotating tapered beam.

3. Results and discussion

The above dynamic stiffness matrix can now be used to compute natural frequencies and mode shapes of either a single rotating tapered beam or an assembly of them. An accurate and reliable method of applying the dynamic stiffness matrix in free vibration analysis is to use the algorithm of Wittrick and Williams, generally known as the W–W algorithm, which has featured in literally hundreds of papers since its original development [23].

By applying the theory in conjunction with the W–W algorithm, a large set of results for natural frequencies and mode shapes of rotating tapered beams for various boundary conditions was obtained. However, because of space limitation the authors have been selective in the presentation of results by resorting to the practical case of cantilever boundary conditions, which has widespread coverage in the literature.

The following non-dimensional natural frequency (λ_i) and rotational speed parameter (η) are defined:

$$\lambda_i = \omega_i/\omega_0, \ \eta = \Omega/\omega_0, \tag{50}$$

where the ith natural frequency ω_i, and the rotational speed Ω are non-dimensionalised with respect to ω_0, which is given by

$$\omega_0 = \sqrt{\frac{\mathrm{EI}_0}{m_0 L^4}}. \tag{51}$$

Results are given for both types of tapered beam whose profiles are uniquely defined by the integer n which can be either 1 or 2. In particular, the effects of rotational speed parameter (η), taper ratio (c), and hub radius ratio (r_H/L) on the non-dimensional natural frequencies (λ_i) are investigated.

For the two values of n (1 and 2) Fig. 5 shows the variation of the first four non-dimensional natural frequencies with rotational speed parameter for the tapered beam when $c = 0.5$ and $r_H/L = 0$. The solid and broken lines represent the two cases $n = 1$ and 2, respectively. The figure shows an increasing trend of the non-dimensional natural frequencies with the rotational speed parameter as expected. Although each of λ_i for the two cases looks very close to each other, the actual natural frequencies, see Eqs. (50) and (51), can be markedly different. For validation purposes, a set of natural frequencies computed for a range of rotational speed parameters for the two types of tapered beam is shown up to six-figure accuracy in Table 1. The results for the case $n = 1$ agreed completely with the exact ones reported by Hodges and Rutkowski [7]. However, the results for the case $n = 2$ reported by Khulief [8] did not agree with the ones in Table 1. Representative results from

Ref. [8] for the case when $\eta = 10$ are shown bold in parenthesis (see last row and columns 7–11 of Table 1). Clearly, there are considerable differences (around 25% in the fundamental) between the results from the present theory and those reported by Khulief (see Table 7 of Ref. [8]). This anomaly prompted a further investigation by the present authors who idealised the tapered beam (for the case $n = 2$) by discretising it into 20 and 50 uniform beams, respectively, so as to represent the tapered beam as a stepped beam. This approach is similar to that used in Ref. [4] which showed that the parabolic limit of the approximate results (using different number of uniform elements to represent the tapered beam) gives accurate results. For a taper ratio $c = 0.5$ and for two different rotational speed parameters $\eta = 5$ and 10, Table 2 shows approximate results using 20 and 50 uniform elements (N) and their parabolic limit. The approximate results of Table 2 are in good agreement with the corresponding results of Table 1 and importantly, the parabolic limit of the approximate results agreed accurately (up to five significant figures!) with the exact results. (Note that if the parabolic limit is not used, around 500 uniform elements will be needed to obtain a five-figure accuracy.) The authors, nevertheless, sought an independent confirmation of the correctness of their results. Hodges and Rutkowski [7] did not present results for the case $n = 2$, but they developed the necessary theory and computer programs to analyse this particular case. At the authors' request, the first author of Ref. [7] provided the required results,

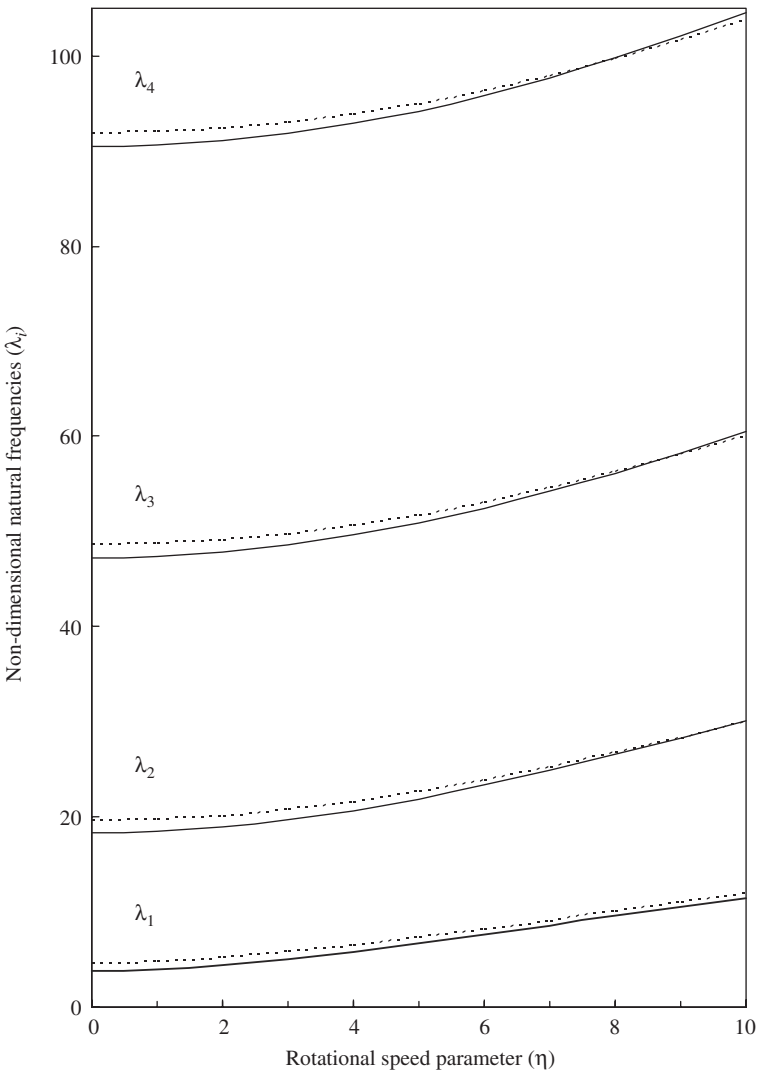

Fig. 5. The effect of rotational speed parameter on the first four non-dimensional natural frequencies of a rotating tapered cantilever beam with $c = 0.5$ and $r_H/L = 0$. ——————— $n = 1$, - - - - - - - - - - - - - - - - - - - $n = 2$.

Table 1
The effect of rotational speed parameter (η) on the non-dimensional natural frequencies (λ_i) for a rotating cantilever beam with $c = 0.5$ and $r_H/L = 0$

η	$n = 1$					$n = 2$				
	λ_1	λ_2	λ_3	λ_4	λ_5	λ_1	λ_2	λ_3	λ_4	λ_5
0	3.82379	18.3173	47.2648	90.4505	148.002	4.62515	19.5476	48.5789	91.8128	149.390
1	3.98661	18.4740	47.4173	90.6039	148.156	4.76405	19.6803	48.7073	91.9409	149.518
2	4.43680	18.9366	47.8717	91.0625	148.619	5.15641	20.0733	49.0906	92.3243	149.903
3	5.09267	19.6839	48.6190	91.8216	149.386	5.74578	20.7121	49.7227	92.9597	150.542
4	5.87877	20.6851	49.6456	92.8730	150.454	6.47262	21.5749	50.5938	93.8415	151.431
5	6.74340	21.9053	50.9338	94.2064	151.814	7.29014	22.6360	51.6918	94.9627	152.567
6	7.65514	23.3093	52.4632	95.8090	153.460	8.16630	23.8684	53.0018	96.3142	153.942
7	8.59557	24.8647	54.2124	97.6666	155.380	9.08036	25.2461	54.5082	97.8861	155.552
8	9.55396	26.5437	56.1595	99.7638	157.564	10.0192	26.7454	56.1941	99.6673	157.387
9	10.5239	28.3227	58.2833	102.084	160.001	10.9747	28.3459	58.0434	101.646	159.439
10	11.5015	30.1827	60.5639	104.612	162.677	11.9415	30.0299	60.0399	103.810	161.701
						(**8.93378**)	(**25.3048**)	(**55.0124**)	(**98.6147**)	(**156.494**)

Results from Ref. [8] for the case when $n = 2$ and $\eta = 10$ are shown bold in parenthesis.

Table 2
The first five non-dimensional natural frequencies for a rotating tapered cantilever beam for the case $n = 2$ with $c = 0.5$ and $r_H/L = 0$ using uniform-element idealization

$\lambda_i = \omega_i\sqrt{m_0L^4/\mathrm{EI}_0}$	$\eta = 5$			$\eta = 10$		
	$N = 20$	$N = 50$	Parabolic limit	$N = 20$	$N = 50$	Parabolic limit
λ_1	7.28411	7.28918	7.29014	11.9352	11.9405	11.9415
λ_2	22.5994	22.6301	22.6360	29.9980	30.0248	30.0299
λ_3	51.5892	51.6754	51.6917	59.9458	60.0247	60.0397
λ_4	94.7626	94.9303	94.9623	103.620	103.779	103.809
λ_5	152.237	152.513	152.566	161.383	161.649	161.699

and confirmed the correctness of the current theory. The results from this independent investigation which agreed completely with the results obtained from the present theory were communicated to the authors by a private (e-mail) communication [22].

Fig. 6 illustrates the effects of taper ratio on the first three non-dimensional natural frequencies of the tapered beam for both $n = 1$ and 2 when r_H/L is zero, and η is set to 0 and 5, respectively. For interested readers who wish to cheque their own theories or computer programs based on the equations given in this paper, Tables 3 and 4 provide numerical results for the two cases, respectively. The results demonstrate the effects of both taper ratio and rotational speed parameter on the non-dimensional natural frequencies.

The next set of results was obtained to demonstrate the effect of hub radius ratio on the non-dimensional natural frequencies of the tapered beam. Fig. 7 illustrates this effect for both $n = 1$ and 2, when η and c are set to 5 and 0.5, respectively. The non-dimensional natural frequencies increase with the hub radius ratio as expected because of the increase in centrifugal stiffening of the beam and the results are in accord with earlier investigations [9,11].

Another set of results was obtained to illustrate some representative mode shapes of the rotating tapered beam. Fig. 8 shows the first five non-dimensional natural frequencies and normalised mode shapes of the two types of the rotating tapered beam for which the values of c, η and r_H/L were set to 0.5, 5.0 and 0.0, respectively. It is interesting to note that for this particular case, the non-dimensional natural frequencies and the corresponding normalised mode shapes for the two types of a tapered beam are similar. This is not unexpected in view of Eqs. (1) and (2), which show that for any value of c, the corresponding ratio of the

bending rigidity EI(y) and the mass per unit length $m(y)$ at any cross-section of the tapered beam is exactly the same for both $n = 1$ and 2.

4. Scope and limitations of the theory

The theory developed in this paper is intended to be used for free vibration analysis of rotating tapered beams within the range of taper ratio $0 < c < 1$. Results have been presented in the previous section for practical values of c, which lie between 0.1 and 0.8.

For the special case when $c = 0$, the tapered beam reduces to a uniform one, see Eqs. (1) and (2), and the present theory cannot be used because of numerical overflow resulting from division by zero, see Eq. (13). In this case, the simpler dynamic stiffness theory developed earlier by Banerjee [4] can be used. However, the present theory will allow the use of small values of c close to zero (say, 10^{-3} or 10^{-4}) to obtain results for rotating uniform beams within reasonable accuracy.

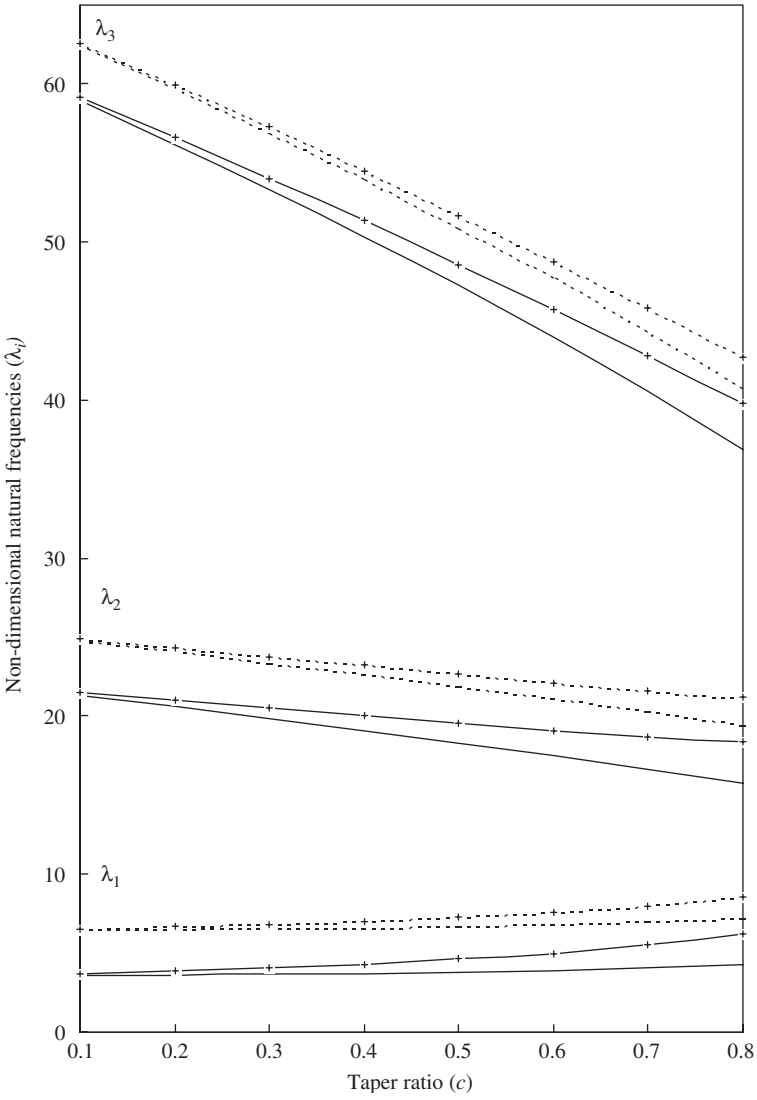

Fig. 6. The effect of taper ratio on the first three non-dimensional natural frequencies of a rotating tapered cantilever beam with $r_H/L = 0$. — ($n = 1$, $\eta = 0$), — + — ($n = 2$, $\eta = 0$), ----- ($n = 1$, $\eta = 5$), ---- + ---- ($n = 2$, $\eta = 5$).

Table 3
The effect of taper ratio (c) and rotational speed parameter (η) on the non-dimensional natural frequencies (λ_i) for a rotating tapered cantilever beam for the case $n = 1$ with $r_H/L = 0$

c	$\eta = 0$			$\eta = 5$			$\eta = 10$		
	λ_1	λ_2	λ_3	λ_1	λ_2	λ_3	λ_1	λ_2	λ_3
0.1	3.55870	21.3381	58.9799	6.49115	24.7805	62.5113	11.2455	32.9968	71.9834
0.2	3.60827	20.6210	56.1923	6.53913	24.0961	59.7504	11.2950	32.3325	69.2537
0.3	3.66675	19.8806	53.3222	6.59525	23.3906	56.9112	11.3523	31.6445	66.4503
0.4	3.73708	19.1138	50.3537	6.66206	22.6612	53.9789	11.4200	30.9292	63.5598
0.5	3.82379	18.3173	47.2649	6.74340	21.9053	50.9338	11.5015	30.1827	60.5639
0.6	3.93428	17.4878	44.0248	6.84537	21.1207	47.7478	11.6023	29.4013	57.4379
0.7	4.08171	16.6252	40.5879	6.97848	20.3086	44.3805	11.7314	28.5839	54.1459
0.8	4.29249	15.7427	36.8846	7.16281	19.4848	40.7725	11.9055	27.7441	50.6370
0.9	4.63073	14.9308	32.8331	7.44359	18.7412	36.8667	12.1592	26.9695	46.8737

Table 4
The effect of taper ratio (c) and rotational speed parameter (η) on the non-dimensional natural frequencies (λ_i) for a rotating cantilever beam for the case $n = 2$ with $r_H/L = 0$

c	$\eta = 0$			$\eta = 5$			$\eta = 10$		
	λ_1	λ_2	λ_3	λ_1	λ_2	λ_3	λ_1	λ_2	λ_3
0.1	3.67370	21.5503	59.1886	6.56330	24.9029	62.6152	11.3017	32.9554	71.8405
0.2	3.85511	21.0568	56.6303	6.69693	24.3478	59.9763	11.4188	32.2499	68.9817
0.3	4.06694	20.5555	54.0152	6.85629	23.7820	57.2815	11.5589	31.5243	66.0667
0.4	4.31878	20.0500	51.3346	7.04980	23.2088	54.5230	11.7295	30.7818	63.0887
0.5	4.62515	19.5476	48.5789	7.29014	22.6360	51.6918	11.9415	30.0299	60.0399
0.6	5.00904	19.0649	45.7384	7.59724	22.0803	48.7797	12.2119	29.2867	56.9143
0.7	5.50926	18.6412	42.8104	8.00426	21.5823	45.7866	12.5679	28.5962	53.7154
0.8	6.19639	18.3855	39.8336	8.56998	21.2521	42.7558	13.0550	28.0752	50.4956
0.9	7.20488	18.6803	37.1241	9.40214	21.4620	40.0150	13.7492	28.0900	47.6075

Another special case arises when $c = 1$, see Eqs. (1) and (2). At this limiting value of c the thin end of the beam converges to a sharp point and the present theory will cause numerical ill-conditioning and hence cannot be used. Of course, $c = 1$ is a theoretical limit which can never be reached in practice. It is well known that the elastic critical buckling load of such a point-ended beam is zero [24,25]. However, the free vibration analysis of such a point-ended beam in the absence of any axial load has been reported in Ref. [26]. The present theory can be used to obtain an approximate result for this case by using a taper ratio close to unity. For both $n = 1$ and 2, and for cantilever end-condition at the thick end of the beam, Table 5 shows results for $c = 0.99$ and 0.995 for hub radius ratio $r_H/L = 0$ when the rotational speed parameter η is set to 0 and 5, respectively. The results converge almost parabolically as the value of c increases towards unity. Thus, the result for $c = 1$ can be extrapolated by establishing the parabolic limit of the two sets of results obtained using $c = 0.99$ and 0.995. As shown in Table 5, the parabolic limits of the results for the non-rotating beam are in close agreement with the ones reported in Ref. [26], which are shown bold in the parenthesis. Comparison of natural frequencies for the rotating tapered beam with $c = 1$ has not been possible because to the best of the authors' knowledge no specimen results could be found in the literature.

5. Conclusions

The free vibration problem of a rotating tapered beam is investigated by developing its dynamic stiffness matrix, and then using it in conjunction with the W–W algorithm. The type of taper considered covers a large

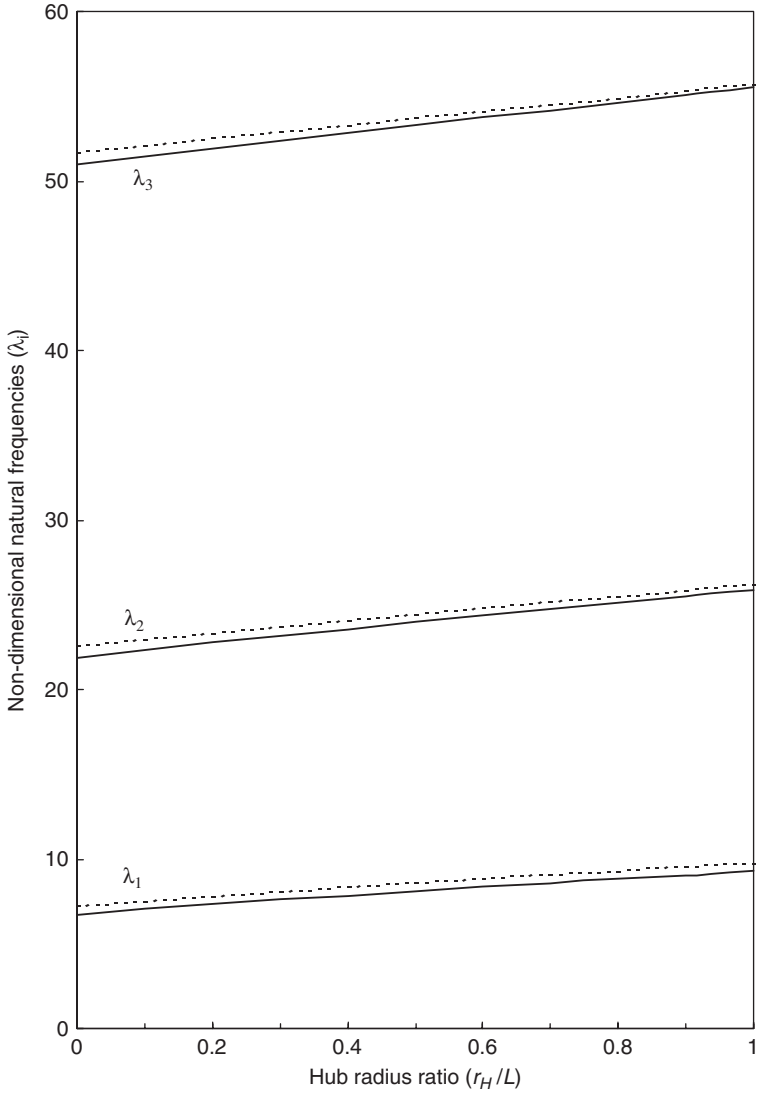

Fig. 7. The effect of hub radius ratio on the first three non-dimensional natural frequencies of the rotating tapered cantilever beam with $\eta = 5$ and $c = 0.5$. ——————— $n = 1$, ····· $n = 2$.

number of practical cases. A detailed set of numerical results is presented and some inaccuracies in published results are corrected. It is intended that the numerical results of this paper will constitute benchmark answers to some of the free vibration problems of rotating tapered beams. An extension of the dynamic stiffness theory to a rotating tapered Timoshenko beam will be considerably more difficult because unlike rotating uniform Timoshenko beams, the two differential equations governing the bending displacement and bending rotation will be very different.

Acknowledgements

The authors are grateful to Adam Sobey and Peter Daniels of City University, London and Dewey Hodges of Gerogia Institute of Technology, Atlanta, USA for help given them during this research. The work was supported by EPSRC (Grant Ref GR/R21875/01), UK.

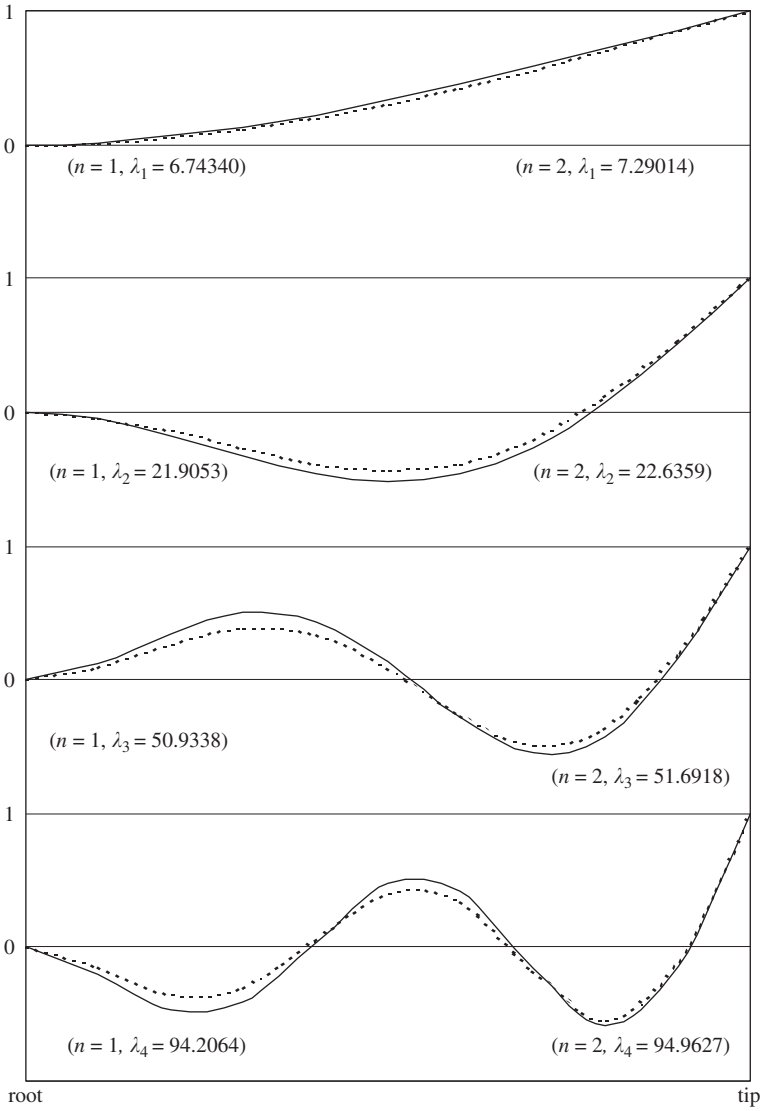

Fig. 8. Non-dimensional natural frequencies and normalised mode shapes of a rotating tapered cantilever beam with $c = 0.5$, $\eta = 5$, and $r_H/L = 0$. ——— $n = 1$, ····· $n = 2$.

Appendix A

Elements of **Q** matrix of Eq. (47).

A.1. Tapered beam with profile defined by n = 1

$$
\begin{aligned}
q_{11} &= R_3\{6a_4(0) - 6a_3(0) + (\bar{C}_1 + \bar{C}_2 + \bar{C}_4)a_2(0)\},\\
q_{12} &= R_3\{6a_3(1) - 6a_2(1) + (\bar{C}_1 + \bar{C}_2 + \bar{C}_4)a_1(1)\},\\
q_{13} &= 6R_3\{a_2(2) - a_1(2)\},\ q_{14} = 6R_3a_1(3),\\
q_{21} &= -2R_2a_3(0),\ q_{22} = -2R_2a_2(1),\ q_{23} = -2R_2a_1(2),\ q_{24} = 0,
\end{aligned}
$$

Table 5
The first four non-dimensional natural frequencies (λ_i) for the limiting case of the cantilever beam when the taper ratio c approaches unity for $n = 1$, 2 and $\eta = 0$, 5 with $r_H/L = 0$

λ_i	$\eta = 0$						$\eta = 5$					
	$n = 1$			$n = 2$			$n = 1$			$n = 2$		
	$c = 0.99$	$c = 0.995$	Parabolic limit	$c = 0.99$	$c = 0.995$	Parabolic limit	$c = 0.99$	$c = 0.995$	Parabolic limit	$c = 0.99$	$c = 0.995$	Parabolic limit
λ_1	5.21445	5.26337	5.27968 (**5.31510**)	8.54601	8.63232	8.66108 (**8.71926**)	7.88549	7.92027	7.93186	11.3152	10.5751	10.3284
λ_2	14.9670	15.0722	15.1072 (**15.2072**)	20.7301	20.9355	21.0039 (**21.1457**)	18.7634	18.8496	18.8783	25.2964	23.4844	22.8804
λ_3	29.7265	29.8064	29.8330 (**30.0198**)	37.7253	38.0742	38.1905 (**38.4538**)	33.9491	34.0209	34.0448	42.8012	40.8575	40.2096
λ_4	49.6986	49.5473	49.4969 (**49.7633**)	59.6278	60.0908	60.2451 (**60.6801**)	54.1093	53.9691	53.9224	64.0785	62.9906	62.6280

Results from Ref. [26] are shown bold in parenthesis.

$$
\begin{aligned}
q_{3i} = & -R_3[(1-c)^3 f'''(c,\ i-1) - 3(1-c)^2 f''(c,\ i-1) \\
& + \{\bar{C}_1(1-c)^3 + \bar{C}_2(1-c)^2 + \bar{C}_4\} f'(c,\ i-1)], \\
q_{4i} = & R_2(1-c)^3 f''(c,\ i-1).
\end{aligned} \tag{A.1}
$$

A.2. Tapered beam with profile defined by $n = 2$

$$
\begin{aligned}
q_{11} &= R_3\{6a_4(0) - 8a_3(0) + (\bar{C}_1 + \bar{C}_2 + \bar{C}_4)a_2(0)\}, \\
q_{12} &= R_3\{6a_3(1) - 8a_2(1) + (\bar{C}_1 + \bar{C}_2 + \bar{C}_4)a_1(1)\}, \\
q_{13} &= R_3\{6a_2(2) - 8a_1(2)\},\ q_{14} = 6R_3 a_1(3), \\
q_{21} &= -2R_2 a_3(0),\ q_{22} = -2R_2 a_2(1),\ q_{23} = -2R_2 a_1(2),\ q_{24} = 0, \\
q_{3i} &= -R_3[(1-c)^4 f'''(c,\ i-1) - 4(1-c)^3 f''(c,\ i-1) \\
&\quad + \{\bar{C}_1(1-c)^4 + \bar{C}_2(1-c)^3 + \bar{C}_4\} f'(c,\ i-1)], \\
q_{4i} &= R_2(1-c)^4 f''(c,\ i-1).
\end{aligned} \tag{A.2}
$$

References

[1] S.M. Hashemi, M.J. Richards, Natural frequencies of rotating uniform beams with Coriolis effects, *Transactions of the ASME, Journal of Vibration and Acoustics* 123 (2001) 444–455.

[2] J. Chung, H.H. Yoo, Dynamic analysis of a rotating cantilever beam by using the finite element method, *Journal of Sound and Vibration* 249 (2002) 147–164.

[3] H.H. Yoo, S. Seo, K. Huh, The effect of concentrated mass on the modal characteristics of a rotating cantilever beam, *Proceedings of the Institution of Mechanical Engineers Part C—Journal of Mechanical Engineering Science* 216 (2002) 151–163.

[4] J.R. Banerjee, Free vibration of centrifugally stiffened uniform and tapered beams using the dynamic stiffness method, *Journal of Sound and Vibration* 233 (2000) 857–875.

[5] G. Wang, N.M. Wereley, Free vibration analysis of rotating blades with uniform tapers, *AIAA Journal* 42 (2004) 2429–2437.

[6] K.J. Huang, T.S. Liu, Dynamic analysis of rotating beams with nonuniform cross sections using the dynamic stiffness method, *Transactions of the ASME, Journal of Vibration and Acoustics* 123 (2001) 536–539.

[7] D.H. Hodges, M.J. Rutkowski, Free-vibration analysis of rotating beams by a variable-order finite-element method, *AIAA Journal* 19 (1981) 1459–1466.

[8] Y.A. Khulief, Vibration frequencies of a rotating tapered beam with end mass, *Journal of Sound and Vibration* 134 (1989) 87–97.

[9] W.E. Boyce, R.I. Providence, Effect of hub radius on the vibration of a uniform bar, *Transactions of the ASME, Journal of Applied Mechanics* 23 (1956) 287–290.

[10] D. Pnueli, Natural bending frequency comparable to rotational frequency in rotating cantilever beam, *Transactions of the ASME, Journal of Applied Mechanics* 39 (1972) 602–604.

[11] H. Lo, J.E. Goldberg, J.L. Bogdanoff, Effect of small hub-radius change on bending frequencies of a rotating beam, *Transactions of the ASME, Journal of Applied Mechanics* 27 (1960) 548–550.

[12] L.H. Jones, The transverse vibration of a rotating beam with tip mass: the method of integral equations, *Quarterly of Applied Mechanics* 33 (1975) 193–203.

[13] V.T. Nagaraj, P. Shanthakumar, Rotor blade vibrations by the Galerkin finite element method, *Journal of Sound and Vibration* 43 (1975) 575–577.

[14] R.O. Stafford, V. Giurgiutiu, Semi-analytic methods for rotating Timoshenko beams, *International Journal of Mechanical Sciences* 17 (1975) 719–727.

[15] S. Naguleswaran, Lateral vibration of a centrifugally tensioned uniform Euler–Bernoulli beam, *Journal of Sound and Vibration* 176 (1994) 613–624.

[16] J.R. Banerjee, Dynamic stiffness formulation and free vibration analysis of centrifugally stiffened Timoshenko beams, *Journal of Sound and Vibration* 247 (2001) 97–115.

[17] S.C. Lin, K.M. Hsiao, Vibration analysis of a rotating Timoshenko beam, *Journal of Sound and Vibration* 240 (2001) 303–322.

[18] A. Bazoune, Y.A. Khulief, N.G. Stephen, Further results for modal characteristics of rotating tapered Timoshenko beams, *Journal of Sound and Vibration* 219 (1999) 157–174.

[19] J.R. Banerjee, Dynamic stiffness formulation for structural elements: a general approach, *Computers & Structures* 63 (1997) 101–103.

[20] J.R. Banerjee, F.W. Williams, Exact Bernoulli–Euler dynamic stiffness matrix for a range of tapered beams, *International Journal for Numerical Methods in Engineering* 21 (1985) 2289–2302.

[21] J.R. Banerjee, F.W. Williams, Exact Bernoulli–Euler static stiffness matrix for a range of tapered beam columns, *International Journal for Numerical Methods in Engineering* 23 (1986) 1615–1628.
[22] D.H. Hodges, A private communication, 2004.
[23] W.H. Wittrick, F.W. Williams, A general algorithm for computing natural frequencies of elastic structures, *Quarterly Journal of Mechanics and Applied Mathematics* 24 (1971) 263–284.
[24] F.W. Williams, J.R. Banerjee, Flexural vibration of axially loaded beams with linear or parabolic taper, *Journal of Sound and Vibration* 99 (1985) 121–138.
[25] S.P. Timosheko, J.M. Gere, *Theory of Elastic Stability*, McGraw-Hill Book Company, Inc., New York, 1961.
[26] S. Naguleswaran, A direct solution for the transverse vibration of Euler–Bernoulli wedge and cone beams, *Journal of Sound and Vibration* 172 (1994) 289–304.
[27] H.T.H. Piaggio, *An Elementary Treatise on Differential Equations and their Applications*, CBS Publishers & Distributors, Delhi, 1985.